

Quantum size level structure of narrow-gap semiconductor nanocrystals: Effect of band coupling

Al. L. Efros and M. Rosen

Nanostructure Optics Section, Naval Research Laboratory, Washington, DC 20375

(Received 9 March 1998)

We study the size dependence of electron and hole quantum size levels in spherical semiconductor nanocrystals. An analytical theory of the quantum size levels within a spherical eight-band Pidgeon and Brown model has been developed, which takes into account both the coupling of conduction and valence bands and the complex structure of the valence band in nanocrystals with an infinite potential barrier. We show that in narrow gap semiconductors band mixing must always be taken into account and that it may be important even in wide gap semiconductors, because the mixing is governed by the square root of the ratio of the quantization energy to the energy gap. The strength of the coupling also depends on the ratio of the contributions of remote bands to the effective masses of the electron and the light hole. As a result level structure is very sensitive, in general, to the energy band parameters. The calculated level structure for narrow gap InSb, moderate gap CdTe, and wide gap CdS nanocrystals are presented. [S0163-1829(98)01236-3]

I. INTRODUCTION

The optical properties of nanosize semiconductor crystals have attracted the attention of many investigators because of their potential applications.^{1,2} The ability to tune their absorption and photoluminescence spectra over a very wide range of energy, as much as 1.2 eV, by varying the crystal size opens the opportunity of fabricating nanocrystal based tunable lasers and light-emitting diodes. For example, CdSe nanocrystals have been fabricated with energy gaps varying from 1.8 eV, the bulk value, up to 3 eV, covering the whole visible optical spectrum.³ Another property of these nanocrystals, a strong nonlinear optical response,^{4,5} is important for many applications.

Both linear and nonlinear optical properties of small semiconductor nanocrystals arise as a result of transitions between electron and hole quantum size levels (QSL's). The Coulomb energy of the electron and hole interaction is on the order of $e^2/\kappa a$, where a is the crystal radius and κ is the dielectric constant of the semiconductor. Because the quantization energy increases with decreasing size as $1/a^2$, the Coulomb energy, which grows only as $1/a$, becomes a small correction to the quantization energies of electrons and holes in small crystals, and reduces transition energies by only a relatively small amount. The first theoretical analyses of nanocrystal absorption spectra in this "strong confinement" regime was made using a parabolic approximation to the conduction and valence bands.^{6,7} The absorption spectra obtained are very simple: $\hbar\omega_\nu = E_g + E_\nu^h(a) + E_\nu^e(a) - 1.8e^2/\kappa a$, where E_g is the energy gap, $E_\nu^{h,e}(a) \sim 1/a^2$ are the energies of the ν th hole and electron QSL's, respectively, and the Coulomb correction is calculated in first-order perturbation theory.

However, there are no semiconductors with such simple parabolic conduction and valence bands. Figure 1 shows a band structure typical for semiconductors having cubic or zinc-blende lattice symmetry, e.g., GaAs, InAs, CdSe, CdTe, CdS, or InSb. The conduction band is parabolic only at the bottom of the band. The top of the valence band consists of

a fourfold degenerate subband Γ_8 , describing the dispersion of the light and heavy-hole branches for nonzero k , and the spin-orbit split off subband Γ_7 . The simple parabolic band approximation is useful only for obtaining a qualitative understanding and not for a quantitative description of the optical properties of real semiconductors. The optical properties of small nanocrystals arise from transitions between the QSL's of electrons and holes, but the energies of these levels must be calculated taking into account the real band structure found in these semiconductors.

If one is interested in the behavior of holes only near the top of the valence band, then the Luttinger-Kohn model is adequate. In spherical approximation this model contains only two parameters, γ_1^L and γ^L , which determine the effec-

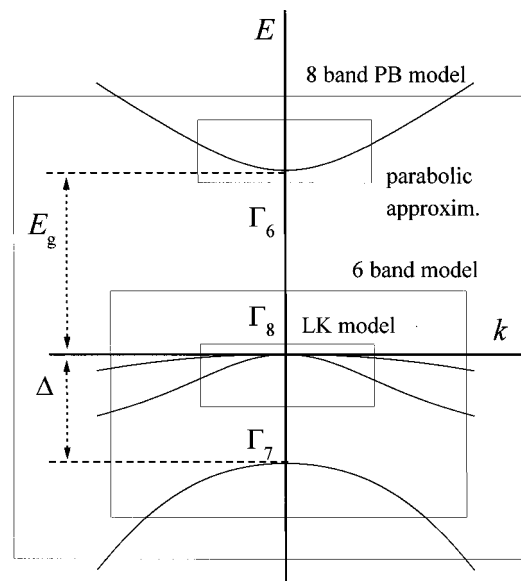


FIG. 1. The bulk band structure of a typical direct gap semiconductor with cubic or zinc-blende lattice structure and band edge at the Γ point of the Brillouin zone. The boxes show the region of applicability of different models used for the calculation of electron and hole QSL's.

tive masses of the light, $m_{lh} = m_0 / (\gamma_1^L + 2\gamma^L)$, and heavy, $m_{hh} = m_0 / (\gamma_1^L - 2\gamma^L)$ holes, respectively, where m_0 is the free-electron mass. Hole levels were calculated within this model in Refs. 8 and 9. However, excited hole levels are not adequately described in this model and we have to take into account all three hole bands: the so-called six-band model. Using the hole levels calculated within this latter model,¹⁰ the excitation spectra of CdSe nanocrystals obtained in absorption,¹¹ hole burning,¹² and photoluminescence excitation experiments^{3,13,14} were described very well. The six-band model, however, does not take the coupling between the conduction and valence bands into account, but considers the confined electron and hole levels as independent. Intuition would say that this is a good approach for wide gap semiconductors, such as CdSe and CdS, but certainly is not appropriate for narrow gap semiconductors where the conduction and valence bands are strongly coupled. A multiband effective-mass approximation appropriate for narrow gap semiconductors was proposed by Pidgeon and Brown¹⁵ (PB) to describe Landau levels in InSb, and was successfully used in all other zinc-blende semiconductors (see, for example, the review by Aggarwal¹⁶). This eight-band model, which simultaneously takes into account the nonparabolicity of the electron- and light-hole dispersion and the complex structure of the valence band, describes the energy band structure around the Γ point of the Brillouin zone very well (see Fig. 1). The importance of this model for the lowest symmetry QSL's in spherical nanocrystals was also shown by Sercel and Vahala.¹⁷ Similar calculations for cubic semiconductors having their band edge at the L point of the Brillouin zone were done by Kang and Wise.¹⁸

In this paper we present a theoretical study of the quan-

tum size level structure of spherical nanocrystals of zinc-blende semiconductors taking into account the mixing of the conduction and valence bands. The calculation is done using the spherical eight-band Luttinger-Kohn Hamiltonian for nanocrystals surrounded by an infinitely high potential barrier. The results of these calculations show that the coupling of the conduction and the valence bands strongly modifies the level structure not only in narrow gap semiconductors, where the spectrum clearly cannot be described without considering the 8-band model, but may also be important in relatively wideband semiconductors (for example, it can change the order of the hole band edge levels in InP).

In Sec. II we examine the spherical eight-band Luttinger-Kohn Hamiltonian and derive equations for the dispersion of electrons and holes and for their radial wave functions. The solutions of the radial equations and analytic expressions for the level energies are given in Sec. III. There we discuss the energy parameters that govern the effect of the conduction band on the hole levels and, conversely, the effect of the valence band on the electron levels. In Sec. IV the size dependence of the QSL's are presented for several semiconductor nanocrystals. Conclusions are drawn in Sec. V.

II. SEPARATION OF VARIABLES

We calculate the positions of the QSL's assuming that the crystals are spherical and neglecting the warping of the valence band connected with the cubic symmetry of the zinc-blende semiconductor lattice structure. The eight-band Luttinger-Kohn Hamiltonian, which describes the electron and hole motion inside the nanocrystal, has the following form in spherical approximation:

	$u_{1/2}^c$	$u_{-1/2}^c$	$u_{3/2,3/2}^v$	$u_{3/2,1/2}^v$	$u_{3/2,-1/2}^v$	$u_{3/2,-3/2}^v$	$u_{1/2,1/2}^v$	$u_{1/2,-1/2}^v$
$u_{1/2}^c$	$E_g + \frac{\alpha}{2m_0} p^2$	0	$\frac{i}{\sqrt{2}} V p_+$	$\sqrt{\frac{2}{3}} V p_z$	$\frac{i}{\sqrt{6}} V p_-$	0	$\frac{i}{\sqrt{3}} V p_z$	$\frac{1}{\sqrt{3}} V p_-$
$u_{-1/2}^c$	0	$E_g + \frac{\alpha}{2m_0} p^2$	0	$-\frac{1}{\sqrt{6}} V p_+$	$i\sqrt{\frac{2}{3}} V p_z$	$-\frac{1}{\sqrt{2}} V p_-$	$\frac{i}{\sqrt{3}} V p_+$	$-\frac{1}{\sqrt{3}} V p_z$
$u_{3/2,3/2}^v$	$-\frac{i}{\sqrt{2}} V p_-$	0	$-(P+Q)$	$-L$	$-M$	0	$-i\sqrt{\frac{1}{2}} L$	$i\sqrt{2} M$
$u_{3/2,1/2}^v$	$\sqrt{\frac{2}{3}} V p_z$	$-\frac{1}{\sqrt{6}} V p_-$	$-L^*$	$-(P-Q)$	0	$-M$	$i\sqrt{2} Q$	$-i\sqrt{\frac{3}{2}} L$
$u_{3/2,-1/2}^v$	$-\frac{i}{\sqrt{6}} V p_+$	$-i\sqrt{\frac{2}{3}} V p_z$	$-M^*$	0	$-(P-Q)$	L	$i\sqrt{\frac{3}{2}} L^*$	$i\sqrt{2} Q$
$u_{3/2,-3/2}^v$	0	$-\frac{1}{\sqrt{2}} V p_+$	0	$-M^*$	L^*	$-(P+Q)$	$i\sqrt{2} M^*$	$i\sqrt{\frac{1}{2}} L^*$
$u_{1/2,1/2}^v$	$-\frac{i}{\sqrt{3}} V p_z$	$-\frac{i}{\sqrt{3}} V p_-$	$i\sqrt{\frac{1}{2}} L^*$	$-i\sqrt{2} Q$	$-i\sqrt{\frac{3}{2}} L$	$-i\sqrt{2} M$	$-\Delta - P$	0
$u_{1/2,-1/2}^v$	$\frac{1}{\sqrt{3}} V p_+$	$-\frac{1}{\sqrt{3}} V p_z$	$-i\sqrt{2} M^*$	$i\sqrt{\frac{3}{2}} L^*$	$-i\sqrt{2} Q$	$-i\sqrt{\frac{1}{2}} L$	0	$-\Delta - P$

(1)

The operators in the Hamiltonian are expressed in terms of projections of the momentum operator, $p_{x,y,z} = -i\hbar\nabla_{x,y,z}$:

$$\begin{aligned} p_{\pm} &= p_x \pm ip_y, & p_{\perp}^2 &= p_x^2 + p_y^2, \\ P &= \frac{\gamma_1}{2m_0} p^2, & Q &= \frac{\gamma}{2m_0} (p_{\perp}^2 - 2p_z^2), \\ L &= \frac{-i\sqrt{3}\gamma}{m_0} p_z p_{-}, & M &= \frac{\sqrt{3}\gamma}{2m_0} p_{-}^2. \end{aligned} \quad (2)$$

The Hamiltonian takes exact account of the coupling between the six valence and two conduction bands, separated by an energy gap E_g . The magnitude of the coupling is described by the Kane matrix element $V = -i\langle S|\hat{p}_z|Z\rangle/m_0$, and Δ is the spin-orbit splitting of the valence band. The Bloch functions of the conduction and valence bands $u_{J,J_z}^{c,v}$, respectively, have the following form:¹⁹

$$\begin{aligned} u_{1/2}^c &= S\uparrow, & u_{3/2,-3/2}^v &= \frac{i}{\sqrt{2}}(X - iY)\downarrow, \\ u_{-1/2}^c &= S\downarrow, & u_{3/2,3/2}^v &= \frac{1}{\sqrt{2}}(X + iY)\uparrow, \\ u_{3/2,1/2}^v &= \frac{i}{\sqrt{6}}[(X + iY)\downarrow - 2Z\uparrow], \\ u_{3/2,-1/2}^v &= \frac{1}{\sqrt{6}}[(X - iY)\uparrow + 2Z\downarrow], \\ u_{1/2,1/2}^v &= \frac{1}{\sqrt{3}}[(X + iY)\downarrow + Z\uparrow], \\ u_{1/2,-1/2}^v &= \frac{i}{\sqrt{3}}[-(X - iY)\uparrow + Z\downarrow], \end{aligned} \quad (3)$$

where J is the Bloch function band-edge angular momentum ($\frac{1}{2}$ for the conduction band, $\frac{3}{2}$ for the heavy- and light-hole bands, and $\frac{1}{2}$ for the split-off band). The PB model takes into account the contribution of the remote bands to the effective masses of the electrons and holes in second-order perturbation theory. The parameter $\alpha = 1 + 2f$ includes a piece $2f$ of the contribution to the electron effective mass. The inverse of the electron effective mass m_c at the bottom of the conduction band includes this contribution and a contribution from the valence band that is expressed in terms of the Kane matrix element and the energy gap:

$$\frac{1}{m_c} = \frac{1}{m_0} \left(\alpha + \frac{E_p}{3} \left[\frac{2}{E_g} + \frac{1}{E_g + \Delta} \right] \right), \quad (4)$$

where $E_p = 2m_0V^2$. The parameters γ_1 and γ account for the contribution of the remote bands to the hole effective masses— L , Q , M , and P include these contributions. The Luttinger parameters of the valence band γ_1^L , γ^L can similarly be written as the sum of contributions from remote bands and from the conduction band:

$$\gamma^L = \gamma + \frac{E_p}{6E_g}, \quad \gamma_1^L = \gamma_1 + \frac{E_p}{3E_g}. \quad (5)$$

Diagonalization of Eq. (1) gives the dispersion of the conduction and valence bands. For the heavy-hole band, we find

$$E_{hh}(p) = (\gamma_1 - 2\gamma)E_K, \quad (6)$$

where $E_K = p^2/2m_0$ is the kinetic energy of a free electron. For the coupled spectra of the other three light hole, spin-orbit hole, and electron bands, the dispersion $E(p)$ is given by the equation

$$\begin{aligned} [E - E_g - \alpha E_K] \{ [E + \gamma_1 E_K + \Delta][E + (\gamma_1 + 2\gamma)E_K] \\ - 8(\gamma E_K)^2 \} - E_p E_K \left(E + \frac{2\Delta}{3} \right) - E_p (\gamma_1 - 2\gamma) E_K^2 = 0. \end{aligned} \quad (7)$$

If one neglects the contribution of the remote bands to the valence band dispersion ($\gamma = 0$, $\gamma_1 = 0$) this equation describes the dispersion of the light holes and electrons in the Kane model:²⁰

$$(E - E_g - \alpha E_K)(E + \Delta)E - E_p E_K(E + 2\Delta/3) = 0. \quad (8)$$

If we take $\alpha = 0$, then for $E < 0$ Eq. (7) gives the dispersion of the light, heavy, and spin-orbit split-off holes in wideband semiconductors, but includes nonparabolicity of the holes (see for comparison Ref. 10):

$$\begin{aligned} [E + \gamma_1^L(E)E_K + \Delta][E + \{\gamma_1^L(E) \\ + 2\gamma^L(E)\}E_K] - 8[\gamma^L(E)E_K]^2 = 0, \end{aligned} \quad (9)$$

where here

$$\gamma^L(E) = \gamma + \frac{E_p}{6(E_g - E)}, \quad \gamma_1^L(E) = \gamma_1 + \frac{E_p}{3(E_g - E)}, \quad (10)$$

[see for comparison Eq. (5)].

The Hamiltonian, Eq. (1), neglects the corrugation of the hole constant-energy surface connected with zinc-blende symmetry of the crystal lattice. This asymmetry is reflected in the difference of the two contributions of remote bands to the hole effective masses: γ_2 and γ_3 . It has been shown that if we take $\gamma = (2\gamma_2 + 3\gamma_3)/5$ then energy levels in any spherical potential are correct to first order in perturbation theory.²¹ The second order correction is usually small because $\gamma_3 - \gamma_2 \ll \gamma_2 + \gamma_3$.

The Hamiltonian in Eq. (1) describes the electron- and hole-energy spectra only if their typical energies are close enough to the bottom of the conduction band and to the top of the valence band. In practice this means that the quantization energy must be smaller than the distance in energy to the next higher (lower) energy extremum in the conduction (valence) band.

In spherical nanocrystals each electron and hole state is characterized by its parity (\pm), total angular momentum $j = J + L$, where L is the envelope angular momentum, and the projection of the total angular momentum $m = j_z$. The wave functions of these states can be written as a linear expansion in the eight Bloch functions:

$$\psi_{j,m}^{\pm}(\mathbf{r}) = R_c(r)^{\pm} \sum_{\mu=-1/2}^{1/2} \Omega_{\mu}^c u_{\mu}^c + \sum_{i=1,2} R_{hi}^{\pm}(r) \sum_{\mu=-3/2}^{3/2} \Omega_{\mu}^{hi} u_{3/2,\mu}^v + R_s(r)^{\pm} \sum_{\mu=-1/2}^{1/2} \Omega_{\mu}^s u_{1/2,\mu}^v. \quad (11)$$

An explicit analytical angular representation of the Ω functions is given in Ref. 22. For the even states,

$$\Omega^c = \begin{pmatrix} \sqrt{\frac{j+m}{2j}} Y_{j-1/2,m-1/2} \\ \sqrt{\frac{j-m}{2j}} Y_{j-1/2,m+1/2} \end{pmatrix},$$

$$\Omega^{h1} = N_1 \begin{pmatrix} \sqrt{3(j+m)(j-m+1)(j-m+2)} Y_{j+1/2,m-3/2} \\ i(j+3m) \sqrt{(j-m+1)} Y_{j+1/2,m-1/2} \\ (j-3m) \sqrt{(j+m+1)} Y_{j+1/2,m+1/2} \\ i \sqrt{3(j-m)(j+m+1)(j+m+2)} Y_{j+1/2,m+3/2} \end{pmatrix}, \quad (12)$$

$$\Omega^{h2} = N_2 \begin{pmatrix} -\sqrt{(j+m)(j+m-1)(j+m-2)} Y_{j-3/2,m-3/2} \\ i \sqrt{3(j-m)(j+m-1)(j+m)} Y_{j-3/2,m-1/2} \\ \sqrt{3(j+m)(j-m)(j-m-1)} Y_{j-3/2,m+1/2} \\ -i \sqrt{(j-m)(j-m-1)(j-m-2)} Y_{j-3/2,m+3/2} \end{pmatrix},$$

$$\Omega^s = \begin{pmatrix} \sqrt{\frac{j-m+1}{2(j+1)}} Y_{j+1/2,m-1/2} \\ -i \sqrt{\frac{j+m+1}{2(j+1)}} Y_{j+1/2,m+1/2} \end{pmatrix}, \quad (13)$$

where $N_1 = 1/\sqrt{2j(2j+2)(2j+3)}$, $N_2 = 1/\sqrt{2j(2j-1)(2j-2)}$, and the $Y_{l,m}(\theta, \varphi)$ are spherical harmonics as defined in Edmonds.²³ (Note: Using alternative definitions of $Y_{l,m}(\theta, \varphi)$ leads to alternative expressions for the wave function.) Substituting these functions into Eq. (1), we obtain four coupled second-order differential equations for the radial functions $R_{c,h1,h2,s}^+(r)$ of the even states:

$$[\varepsilon_g - \varepsilon - \alpha \Delta_{j-1/2}] R_c^+ + \frac{v}{\sqrt{6}} \sqrt{1+3\eta_j^+} A_{j+1/2}^- R_{h1}^+ - \frac{v}{\sqrt{2}} \sqrt{1-\eta_j^+} A_{j-3/2}^+ R_{h2}^+ + \frac{v}{\sqrt{3}} A_{j+1/2}^- R_s^+ = 0,$$

$$\frac{v}{\sqrt{6}} \sqrt{1+3\eta_j^+} A_{j-1/2}^+ R_c^+ + [[\gamma_1 - \gamma(1-3\eta_j^+)] \Delta_{j+1/2} - \varepsilon] R_{h1}^+$$

$$+ \gamma \sqrt{3[1+2\eta_j^+ - 3(\eta_j^+)^2]} A_{j-3/2}^+ R_{h2}^+ + \gamma \sqrt{2(1+3\eta_j^+)} \Delta_{j+1/2} R_s^+ = 0,$$

$$- \frac{v}{\sqrt{2}} \sqrt{1-\eta_j^+} A_{j-1/2}^- R_c^+ + \gamma \sqrt{3[1+2\eta_j^+ - 3(\eta_j^+)^2]} A_{j+1/2}^- R_{h1}^+ + [[\gamma_1 + \gamma(1-3\eta_j^+)] \Delta_{j-3/2} - \varepsilon] R_{h2}^+$$

$$+ \gamma \sqrt{6(1-\eta_j^+)} A_{j+1/2}^- R_s^+ = 0,$$

$$\frac{v}{\sqrt{3}} A_{j-1/2}^+ R_c^+ + \gamma \sqrt{2(1+3\eta_j^+)} \Delta_{j+1/2} R_{h1}^+ + \gamma \sqrt{6(1-\eta_j^+)} A_{j-3/2}^+ R_{h2}^+ + [\gamma_1 \Delta_{j+1/2} - \delta - \varepsilon] R_s^+ = 0, \quad (14)$$

where $\eta_j^+ = 1/2j$, $\varepsilon_g = 2m_0 E_g / \hbar^2$, $\delta = 2m_0 \Delta / \hbar^2$, $v = 2m_0 V / \hbar$, $\varepsilon = 2m_0 E / \hbar^2$, and E is the energy of the state. The operators

$$A_l^+ = -\frac{\partial}{\partial r} + \frac{l}{r}, \quad A_l^- = \frac{\partial}{\partial r} + \frac{l+1}{r}, \quad (15)$$

are raising and lowering operators for spherical Bessel functions, $j_l(r)$: $A_l^+ j_l(r) = j_{l+1}(r)$, and $A_l^- j_l(r) = j_{l-1}(r)$; $A_l^{+2} = A_{l+1}^+ A_l^+$, $A_l^{-2} = A_{l-1}^- A_l^-$, and Δ_l is the Laplacian

$$\Delta_l = \frac{\partial^2}{\partial r^2} + \frac{2}{r} \frac{\partial}{\partial r} - \frac{l(l+1)}{r^2}. \quad (16)$$

Correspondingly, for the odd states the angular wave functions $\Omega^{c,h1,h2,s}$ can be written

$$\Omega^c = \begin{pmatrix} -\sqrt{\frac{j-m+1}{2j+2}} Y_{j+1/2,m-1/2} \\ \sqrt{\frac{j+m+1}{2j+2}} Y_{j+1/2,m+1/2} \end{pmatrix},$$

$$\Omega^{h1} = N_1 \begin{pmatrix} \sqrt{3(j+m)(j-m+1)(j+m-1)} Y_{j-1/2,m-3/2} \\ -i(j-3m+1)\sqrt{(j+m)} Y_{j-1/2,m-1/2} \\ (j+3m+1)\sqrt{(j-m)} Y_{j-1/2,m+1/2} \\ -i\sqrt{3(j+m+1)(j-m)(j-m-1)} Y_{j-1/2,m+3/2} \end{pmatrix}, \quad (17)$$

$$\Omega^{h2} = N_2 \begin{pmatrix} -\sqrt{(j-m+1)(j-m+2)(j-m+3)} Y_{j+3/2,m-3/2} \\ -i\sqrt{3(j+m+1)(j-m+2)(j-m+1)} Y_{j+3/2,m-1/2} \\ \sqrt{3(j-m+1)(j+m+1)(j+m+2)} Y_{j+3/2,m+1/2} \\ i\sqrt{(j+m+1)(j+m+2)(j+m+3)} Y_{j+3/2,m+3/2} \end{pmatrix},$$

$$\Omega^s = \begin{pmatrix} \sqrt{\frac{j+m}{2j}} Y_{j-1/2,m-1/2} \\ i\sqrt{\frac{j-m}{2j}} Y_{j-1/2,m+1/2} \end{pmatrix},$$

where $N_1 = 1/\sqrt{2j(2j+2)(2j-1)}$ and $N_2 = 1/\sqrt{2(j+1)(2j+3)(2j+4)}$. Substituting these functions into Eq. (1), we obtain four coupled second-order differential equations for the radial functions $R_{c,h1,h2,s}^-(r)$ of the odd states:

$$[\varepsilon_g - \varepsilon - \alpha\Delta_{j+1/2}]R_c^- - \frac{\nu}{\sqrt{6}}\sqrt{1-3\eta_j^-}A_{j-1/2}^+R_{h1}^- + \frac{\nu}{\sqrt{2}}\sqrt{1+\eta_j^-}A_{j+3/2}^-R_{h2}^- + \frac{\nu}{\sqrt{3}}A_{j-1/2}^+R_s^- = 0,$$

$$-\frac{\nu}{\sqrt{6}}\sqrt{1-3\eta_j^-}A_{j+1/2}^-R_c^- + [[\gamma_1 - \gamma(1+3\eta_j^-)]\Delta_{j-1/2} - \varepsilon]R_{h1}^-$$

$$+ \gamma\sqrt{3[1-2\eta_j^- - 3(\eta_j^-)^2]}A_{j+3/2}^-R_{h2}^- - \gamma\sqrt{2(1-3\eta_j^-)}\Delta_{j-1/2}R_s^- = 0, \quad (18)$$

$$\frac{\nu}{\sqrt{2}}\sqrt{1+\eta_j^-}A_{j+1/2}^+R_c^- + \gamma\sqrt{3[1-2\eta_j^- - 3(\eta_j^-)^2]}A_{j-1/2}^+R_{h1}^- + [[\gamma_1 + \gamma(1+3\eta_j^-)]\Delta_{j+3/2} - \varepsilon]R_{h2}^- - \gamma\sqrt{6(1+\eta_j^-)}A_{j-1/2}^+R_s^- = 0,$$

$$\frac{\nu}{\sqrt{3}}A_{j+1/2}^-R_c^- - \gamma\sqrt{2(1-3\eta_j^-)}\Delta_{j-1/2}R_{h1}^- - \gamma\sqrt{6(1+\eta_j^-)}A_{j+3/2}^-R_{h2}^- + [\gamma_1\Delta_{j-1/2} - \delta - \varepsilon]R_s^- = 0,$$

where $\eta_j^- = 1/(2j+2)$. In each set [Eqs. (14) and (18)] three of the equations, for radial functions $R_{h1,h2,s}$ connected with the valence band, are similar to those obtained for the valence band states in the six-band model.¹⁰ The additional equation describes the direct coupling between the conduction and the valence bands.

It will be convenient, later in the paper, to use the stan-

dard atomic notation for the electron and hole QSLs that are solutions of Eqs. (14) and (16): nQ_j where j is the total angular momentum, $Q=S,P,D,\dots$ denotes the spectroscopic notation for the lowest value of L in the wave functions, described by Eqs. (12) and (17), and n is the ordinal number of the level with a given symmetry.^{11,3} The interband selection rules follow from the angular dependence of the

wave functions. The only allowed transitions are from $nS_j(h)$ hole states to $kS_{j'}(e)$ electron states, from $nP_j(h)$ hole states to $kP_{j'}(e)$ electron states, etc.^{11,3}

III. QUANTUM SIZE LEVELS AND WAVE FUNCTIONS

A. General expressions

1. Even states

Noting that the operators A_l^\pm are raising and lowering operators for spherical Bessel functions $j_l(x)$ and that the radial Laplacian Δ_l just changes the sign of $j_l(x)$, one can

express the solutions of the set of coupled differential Eqs. (14) and (18) inside the nanocrystal, for any arbitrary energy, in the form of spherical Bessel functions. For the even states,

$$R_{c,j}^+(r) = C_{c,j}^+ j_{j-1/2}(kr), \quad R_{h1,j}^+(r) = C_{h1,j}^+ j_{j+1/2}(kr),$$

$$R_{h2,j}^+(r) = C_{h2,j}^+ j_{j-3/2}(kr), \quad R_{s,j}^+(r) = C_{s,j}^+ j_{j+1/2}(kr). \quad (19)$$

Upon substituting these into Eq. (14), one finds that coefficients C^+ are the solutions of the system of linear equations:

$$[\varepsilon_g - \varepsilon + \alpha k^2] C_{c,j}^+ + \frac{vk\sqrt{1+3\eta_j^+}}{\sqrt{6}} C_{h1,j}^+ - \frac{vk\sqrt{1-\eta_j^+}}{\sqrt{2}} C_{h2,j}^+ + \frac{vk}{\sqrt{3}} C_{s,j}^+ = 0,$$

$$\frac{vk\sqrt{1+3\eta_j^+}}{\sqrt{6}} C_{c,j}^+ - \{[\gamma_1 - \gamma(1-3\eta_j^+)]k^2 + \varepsilon\} C_{h1,j}^+ + \gamma k^2 \sqrt{3+6\eta_j^+ - 9(\eta_j^+)^2} C_{h2,j}^+ - \gamma k^2 \sqrt{2+6\eta_j^+} C_{s,j}^+ = 0,$$

$$- \frac{vk\sqrt{1-\eta_j^+}}{\sqrt{2}} C_{c,j}^+ + \gamma k^2 \sqrt{3+6\eta_j^+ - 9(\eta_j^+)^2} C_{h1,j}^+ - \{[\gamma_1 + \gamma(1-3\eta_j^+)]k^2 + \varepsilon\} C_{h2,j}^+ + \gamma k^2 \sqrt{6-6\eta_j^+} C_{s,j}^+ = 0,$$

$$\frac{vk}{\sqrt{3}} C_{c,j}^+ - \gamma k^2 \sqrt{2+6\eta_j^+} C_{h1,j}^+ + \gamma k^2 \sqrt{6-6\eta_j^+} C_{h2,j}^+ - [\gamma_1 k^2 + \delta + \varepsilon] C_{s,j}^+ = 0. \quad (20)$$

The condition for there being a nontrivial solution of this system is that its determinant vanishes. It is important to note that, in spite of the fact that the coefficients C^+ depend on j , the determinantal equation *does not* depend on j . The determinantal equation determines the dependence of ε on k and is identical to the dispersion of the electron- and hole-energy spectra in the PB model described by Eqs. (6) and (7), where $k = p/\hbar$. One can turn this around, however, and for each ε find again a quartic equation for k^2 . One solution comes from the dispersion of the heavy holes:

$$k_h^2 = \frac{-\varepsilon}{\gamma_1 - 2\gamma}. \quad (21)$$

A second equation, cubic in k^2 , is connected with the dispersion of the coupled electron, light and spin-orbit split-off hole branches of the quasiparticle spectrum:

$$k^6 + Ak^4 + Bk^2 + C = 0, \quad (22)$$

where

$$A = \frac{v^2}{\alpha(\gamma_1 + 4\gamma)} - \frac{\varepsilon - \varepsilon_g}{\alpha} + \frac{2\varepsilon(\gamma_1 + \gamma) + \delta(\gamma_1 + 2\gamma)}{(\gamma_1 + 4\gamma)(\gamma_1 - 2\gamma)},$$

$$B = \frac{v^2(\varepsilon + 2\delta/3) + \alpha(\varepsilon^2 + \delta\varepsilon)}{\alpha(\gamma_1 + 4\gamma)(\gamma_1 - 2\gamma)}$$

$$- \frac{(\varepsilon - \varepsilon_g)[2\varepsilon(\gamma_1 + \gamma) + \delta(\gamma_1 + 2\gamma)]}{\alpha(\gamma_1 + 4\gamma)(\gamma_1 - 2\gamma)},$$

$$C = - \frac{(\varepsilon - \varepsilon_g)\varepsilon(\varepsilon + \delta)}{\alpha(\gamma_1 + 4\gamma)(\gamma_1 - 2\gamma)}, \quad (23)$$

and gives three more independent solutions k^2 , for each energy. One of the roots of Eq. (22) is much larger than the other two because $v^2 \gg \varepsilon, \varepsilon_g$ (Typically $E_p \sim 20$ eV, while typical energies $E, E_g \sim 2$ eV). To the first order in $\varepsilon, \varepsilon_g$ it can be written

$$k_c^2 \approx -A' = -A + B/A \approx \frac{-v^2}{\alpha(\gamma_1 + 4\gamma)} + \frac{\varepsilon - \varepsilon_g}{\alpha} - \frac{\varepsilon + \delta/3}{(\gamma_1 + 4\gamma)}. \quad (24)$$

The other two roots can be written

$$k_{\pm}^2 = - \frac{B - C/A'}{2A'} \mp \sqrt{\left(\frac{B - C/A'}{2A'}\right)^2 - \frac{C}{A'}}. \quad (25)$$

In general, Eqs. (21) and (22) have four solutions k^2 for each energy. For $k^2 < 0$, k is imaginary and the corresponding Bessel functions are functions of an imaginary argument. As a result, for each ε there are four independent solutions of Eq. (14)—one for each of these k^2 . Expressing the radial wave function as a linear combination of these four independent solutions allows us to satisfy all the boundary conditions for the four component wave function. The solutions of Eq. (14) can be written

$$R_{c,j}^+(r) = C_c^+(cp)j_{j-1/2}(k_cr) + C_c^+(h_-)j_{j-1/2}(k_-r) + C_c^+(h_+)j_{j-1/2}(k_+r),$$

$$R_{h1,j}^+(r) = \frac{v\sqrt{1+3\eta_j^+}}{\sqrt{6}} \left[\frac{k_c\Lambda_h(k_c)C_c^+(cp)j_{j+1/2}(k_cr)}{\Lambda_0(k_c)} + \frac{k_-\Lambda_h(k_-)C_c^+(h_-)j_{j+1/2}(k_-r)}{\Lambda_0(k_-)} + \frac{k_+\Lambda_h(k_+)C_c^+(h_+)j_{j+1/2}(k_+r)}{\Lambda_0(k_+)} \right] + \sqrt{3(1-\eta_j^+)}C_{hh}^+j_{j+1/2}(k_hr),$$

$$R_{h2,j}^+(r) = -\frac{v\sqrt{1-\eta_j^+}}{\sqrt{2}} \left[\frac{k_{cp}\Lambda_h(k_c)C_c^+(cp)j_{j-3/2}(k_cr)}{\Lambda_0(k_c)} + \frac{k_-\Lambda_h(k_-)C_c^+(h_-)j_{j-3/2}(k_-r)}{\Lambda_0(k_-)} + \frac{k_+\Lambda_h(k_+)C_c^+(h_+)j_{j-3/2}(k_+r)}{\Lambda_0(k_+)} \right] + \sqrt{1+3\eta_j^+}C_{hh}^+j_{j-3/2}(k_hr),$$

$$R_{s,j}^+(r) = \frac{v}{\sqrt{3}} \left[\frac{k_c\Lambda_s(k_c)C_c^+(cp)j_{j+1/2}(k_cr)}{\Lambda_0(k_{cp})} + \frac{k_-\Lambda_s(k_-)C_c^+(h_-)j_{j+1/2}(k_-r)}{\Lambda_0(k_-)} + \frac{k_+\Lambda_s(k_+)C_c^+(h_+)j_{j+1/2}(k_+r)}{\Lambda_0(k_+)} \right], \quad (26)$$

where

$$\Lambda_0(k) = (\gamma_1 k^2 + \delta + \varepsilon)[(\gamma_1 + 2\gamma)k^2 + \varepsilon] - 8\gamma^2 k^4,$$

$$\Lambda_h(k) = \delta + \varepsilon + (\gamma_1 - 2\gamma)k^2,$$

$$\Lambda_s(k) = \varepsilon + (\gamma_1 - 2\gamma)k^2. \quad (27)$$

In a nanocrystal with an infinite potential barrier all the components of the wave function must vanish at the crystal surface: $R_{\mu,j}^+(a) = 0$. This condition determines the energy of the electron and hole levels for the even states:

$$\begin{aligned} & -\frac{j_{j-1/2}(k_c a)j_{j+1/2}(k_+ a)k_-k_+\Lambda_h(k_-)\Lambda_s(k_+)}{\Lambda_0(k_-)\Lambda_0(k_+)} \left[j_{j+1/2}(k_- a)j_{j-3/2}(k_h a) + \frac{6j-3}{2j+3}j_{j-3/2}(k_- a)j_{j+1/2}(k_h a) \right] \\ & + \frac{j_{j-1/2}(k_c a)j_{j+1/2}(k_- a)k_-k_+\Lambda_h(k_+)\Lambda_s(k_-)}{\Lambda_0(k_-)\Lambda_0(k_+)} \left[j_{j+1/2}(k_+ a)j_{j-3/2}(k_h a) + \frac{6j-3}{2j+3}j_{j-3/2}(k_+ a)j_{j+1/2}(k_h a) \right] \\ & - \frac{j_{j-1/2}(k_- a)j_{j+1/2}(k_c a)k_c k_+\Lambda_h(k_+)\Lambda_s(k_c)}{\Lambda_0(k_c)\Lambda_0(k_+)} \left[j_{j+1/2}(k_+ a)j_{j-3/2}(k_h a) + \frac{6j-3}{2j+3}j_{j-3/2}(k_+ a)j_{j+1/2}(k_h a) \right] \\ & + \frac{j_{j-1/2}(k_- a)j_{j+1/2}(k_+ a)k_c k_+\Lambda_h(k_c)\Lambda_s(k_+)}{\Lambda_0(k_c)\Lambda_0(k_+)} \left[j_{j+1/2}(k_c a)j_{j-3/2}(k_h a) + \frac{6j-3}{2j+3}j_{j-3/2}(k_c a)j_{j+1/2}(k_h a) \right] \\ & + \frac{j_{j-1/2}(k_+ a)j_{j+1/2}(k_c a)k_c k_-\Lambda_h(k_-)\Lambda_s(k_c)}{\Lambda_0(k_c)\Lambda_0(k_-)} \left[j_{j+1/2}(k_- a)j_{j-3/2}(k_h a) + \frac{6j-3}{2j+3}j_{j-3/2}(k_- a)j_{j+1/2}(k_h a) \right] \\ & - \frac{j_{j-1/2}(k_+ a)j_{j+1/2}(k_- a)k_c k_-\Lambda_h(k_c)\Lambda_s(k_-)}{\Lambda_0(k_c)\Lambda_0(k_-)} \left[j_{j+1/2}(k_c a)j_{j-3/2}(k_h a) + \frac{6j-3}{2j+3}j_{j-3/2}(k_c a)j_{j+1/2}(k_h a) \right] = 0. \end{aligned} \quad (28)$$

For negative k_c^2 , when $\alpha(\gamma_1 + 4\gamma) > 0$, the argument of the spherical Bessel function is imaginary. For negative k^2 we shall always choose the phase of the square root such that $k = +i|k|$, so that $j_j(i|k_c|r) = (i)^j I_j(|k_c|r)$, where $I_j(|k_c|r)$ is the modified spherical Bessel function of the first kind. Using the condition that $|k_c|a \gg 1$ and the asymptotic form for the functions $I_j(x)$, we can simplify Eq. (28):

$$\begin{aligned}
& - \frac{j_{j+1/2}(k_+a)k_-k_+\Lambda_h(k_-)\Lambda_s(k_+)}{\Lambda_0(k_-)\Lambda_0(k_+)} \left[j_{j+1/2}(k_-a)j_{j-3/2}(k_ha) + \frac{6j-3}{2j+3}j_{j-3/2}(k_-a)j_{j+1/2}(k_ha) \right] \\
& + \frac{j_{j+1/2}(k_-a)k_-k_+\Lambda_h(k_+)\Lambda_s(k_-)}{\Lambda_0(k_-)\Lambda_0(k_+)} \left[j_{j+1/2}(k_+a)j_{j-3/2}(k_ha) + \frac{6j-3}{2j+3}j_{j-3/2}(k_+a)j_{j+1/2}(k_ha) \right] \\
& + \frac{j_{j-1/2}(k_-a)|k_c|k_+\Lambda_h(k_+)\Lambda_s(k_c)}{\Lambda_0(k_c)\Lambda_0(k_+)} \left[j_{j+1/2}(k_+a)j_{j-3/2}(k_ha) + \frac{6j-3}{2j+3}j_{j-3/2}(k_+a)j_{j+1/2}(k_ha) \right] \\
& - \frac{j_{j-1/2}(k_-a)j_{j+1/2}(k_+a)|k_c|k_+\Lambda_h(k_c)\Lambda_s(k_+)}{\Lambda_0(k_c)\Lambda_0(k_+)} \left[j_{j-3/2}(k_ha) - \frac{6j-3}{2j+3}j_{j+1/2}(k_ha) \right] \\
& - \frac{j_{j-1/2}(k_+a)|k_c|k_-\Lambda_h(k_-)\Lambda_s(k_c)}{\Lambda_0(k_c)\Lambda_0(k_-)} \left[j_{j+1/2}(k_-a)j_{j-3/2}(k_ha) + \frac{6j-3}{2j+3}j_{j-3/2}(k_-a)j_{j+1/2}(k_ha) \right] \\
& + \frac{j_{j-1/2}(k_+a)j_{j+1/2}(k_-a)|k_c|k_-\Lambda_h(k_c)\Lambda_s(k_-)}{\Lambda_0(k_c)\Lambda_0(k_-)} \left[j_{j-3/2}(k_ha) - \frac{6j-3}{2j+3}j_{j+1/2}(k_ha) \right] = 0.
\end{aligned} \tag{29}$$

Using Eqs. (24) and (27), one can show that

$$\frac{|k_c|\Lambda_s(k_c)}{\Lambda_0(k_c)} \approx \frac{|k_c|\Lambda_h(k_c)}{\Lambda_0(k_c)} \approx -\frac{\alpha}{|\alpha|} \sqrt{\frac{\alpha}{v^2(\gamma_1+4\gamma)}}, \tag{30}$$

and finally obtain

$$\begin{aligned}
& (1+3\eta_j^+) \left[\frac{\Lambda_s(k_-)}{\Lambda_h(k_-)} - \frac{\Lambda_s(k_+)}{\Lambda_h(k_+)} \right] j_{j+1/2}(k_+a)j_{j+1/2}(k_-a)j_{j-3/2}(k_ha) + 3(1-\eta_j^+) \\
& \times j_{j+1/2}(k_ha) \left[\frac{\Lambda_s(k_-)}{\Lambda_h(k_-)} j_{j+1/2}(k_-a)j_{j-3/2}(k_+a) - \frac{\Lambda_s(k_+)}{\Lambda_h(k_+)} j_{j+1/2}(k_+a)j_{j-3/2}(k_-a) \right] \\
& = \frac{\alpha}{|\alpha|} \sqrt{\frac{\alpha}{v^2(\gamma_1+4\gamma)}} \frac{\Lambda_0(k_-)}{k_-\Lambda_h(k_-)} \left\{ (1+3\eta_j^+) \left[1 - \frac{\Lambda_s(k_+)}{\Lambda_h(k_+)} \right] j_{j-1/2}(k_-a)j_{j+1/2}(k_+a)j_{j-3/2}(k_ha) \right. \\
& \left. + 3(1-\eta_j^+)j_{j+1/2}(k_ha)j_{j-1/2}(k_-a) \left[j_{j-3/2}(k_+a) + \frac{\Lambda_s(k_+)}{\Lambda_h(k_+)}j_{j+1/2}(k_+a) \right] \right\} \\
& - \frac{\alpha}{|\alpha|} \sqrt{\frac{\alpha}{v^2(\gamma_1+4\gamma)}} \frac{\Lambda_0(k_+)}{k_+\Lambda_h(k_+)} \left\{ (1+3\eta_j^+) \left[1 - \frac{\Lambda_s(k_-)}{\Lambda_h(k_-)} \right] j_{j-1/2}(k_+a)j_{j+1/2}(k_-a)j_{j-3/2}(k_ha) \right. \\
& \left. + 3(1-\eta_j^+)j_{j-1/2}(k_+a)j_{j+1/2}(k_ha) \left[j_{j-3/2}(k_-a) + \frac{\Lambda_s(k_-)}{\Lambda_h(k_-)}j_{j+1/2}(k_-a) \right] \right\}.
\end{aligned} \tag{31}$$

This is an equation for the QSL's in the conduction band, when $\varepsilon > \varepsilon_g$, and in the valence band, when $\varepsilon < 0$. For hole states, k_-^2 is always positive, but k_+^2 is negative when $|\varepsilon| < \delta$. In this case the argument of the Bessel functions is imaginary. As before, we let $k_+ = +i|k_+|$, so that $j_j(i|k_+|r) = (i)^j I_j(|k_+|r)$. If $\alpha = 0$ the equations become the uncoupled equations of the six-band model,^{10,11} which, however, now take into account nonparabolicity of the light hole [see Eq. (9)]. Of the two terms on the right side of Eq. (31), which describe the valence band coupling with the conduction band, the second one is always much smaller than the first.

For the electron levels, both $k_h^2 < 0$ and $k_+^2 < 0$. Again we write the corresponding spherical Bessel functions in Eq. (31) as $j_j(i|k_{h,+}|a) = (i)^j I_j(|k_{h,+}|a)$. For electron levels with energy $\varepsilon > \varepsilon_g$ the momenta $k_{h,+}$ satisfy the condition $|k_{h,+}|a \gg 1$ for almost all direct semiconductor nanocrystals. We can then use the asymptotic form of the modified spherical Bessel function $I_j(x)$ with the large argument and obtain from Eq. (31) the equation that determines the electron quantum size levels:

$$\begin{aligned}
j_{j-1/2}(k_-a) & = \frac{1}{4(1-\Lambda_s(k_+)/\Lambda_h(k_+))} \frac{\alpha}{|\alpha|} \sqrt{\frac{v^2(\gamma_1+4\gamma)}{\alpha}} \frac{k_-\Lambda_h(k_-)}{\Lambda_0(k_-)} \left\{ j_{j+1/2}(k_-a) \left[\frac{4\Lambda_s(k_-)}{\Lambda_h(k_-)} - (1+3\eta_j^+) \frac{\Lambda_s(k_+)}{\Lambda_h(k_+)} \right] \right. \\
& \left. + 3(1-\eta_j^+) \frac{\Lambda_s(k_+)}{\Lambda_h(k_+)} j_{j-3/2}(k_-a) \right\} + \frac{k_-\Lambda_h(k_-)\Lambda_0(k_+)}{|k_+|\Lambda_0(k_-)\Lambda_h(k_+)} \frac{3}{4(1-\Lambda_s(k_+)/\Lambda_h(k_+))} \\
& \times \left\{ j_{j+1/2}(k_-a) \left[\frac{4}{3} \left(\frac{\Lambda_s(k_-)}{\Lambda_h(k_-)} - 1 \right) + (1-\eta_j^+) \right] + (1-\eta_j^+) j_{j-3/2}(k_-a) \right\}.
\end{aligned} \tag{32}$$

If $\gamma_1 + 4\gamma = 0$, this equation becomes the equation for the uncoupled electron QSL's used in the Ref. 11. The two terms on the right hand side of Eq. (32) describe the effect of the coupling with the valence band. Of these, the second one is always much smaller than the first.

2. Odd states

A similar procedure gives us the solution of Eq. (18) for the odd states. The corresponding solutions can be written:

$$R_{c,j}^-(r) = C_c^-(cp)j_{j+1/2}(k_c r) + C_c^-(h_-)j_{j+1/2}(k_- r) + C_c^-(h_+)j_{j+1/2}(k_+ r),$$

$$R_{h1,j}^-(r) = -\frac{v\sqrt{1-3\eta_j^-}}{\sqrt{6}} \left[\frac{k_c \Lambda_h(k_c) C_c^-(cp)j_{j-1/2}(k_c r)}{\Lambda_0(k_c)} + \frac{k_- \Lambda_h(k_-) C_c^-(h_-)j_{j-1/2}(k_- r)}{\Lambda_0(k_-)} + \frac{k_+ \Lambda_h(k_+) C_c^-(h_+)j_{j-1/2}(k_+ r)}{\Lambda_0(k_+)} \right] \\ + \sqrt{3(1+\eta_j^-)} C_{hh}^- j_{j-1/2}(k_h r),$$

$$R_{h2,j}^-(r) = \frac{v\sqrt{1+\eta_j^-}}{\sqrt{2}} \left[\frac{k_c \Lambda_h(k_c) C_c^-(cp)j_{j+3/2}(k_c r)}{\Lambda_0(k_c)} + \frac{k_- \Lambda_h(k_-) C_c^-(h_-)j_{j+3/2}(k_- r)}{\Lambda_0(k_-)} + \frac{k_+ \Lambda_h(k_+) C_c^-(h_+)j_{j+3/2}(k_+ r)}{\Lambda_0(k_+)} \right] \\ + \sqrt{1-3\eta_j^-} C_{hh}^- j_{j+3/2}(k_h r),$$

$$R_{s,j}^-(r) = \frac{v}{\sqrt{3}} \left[\frac{k_c \Lambda_s(k_c) C_c^-(cp)j_{j-1/2}(k_c r)}{\Lambda_0(k_c)} + \frac{k_- \Lambda_s(k_-) C_c^-(h_-)j_{j-1/2}(k_- r)}{\Lambda_0(k_-)} + \frac{k_+ \Lambda_s(k_+) C_c^-(h_+)j_{j-1/2}(k_+ r)}{\Lambda_0(k_+)} \right]. \quad (33)$$

In nanocrystals with an infinite potential barrier the level positions are determined from the four boundary conditions $R_{\mu,j}^-(a) = 0$. The solubility condition of this set of equations gives us the equation determining the energies of the electron and hole states:

$$+ \frac{j_{j+1/2}(k_c a)j_{j-1/2}(k_+ a)k_- k_+ \Lambda_h(k_-) \Lambda_s(k_+)}{\Lambda_0(k_-) \Lambda_0(k_+)} \left[j_{j+3/2}(k_- a)j_{j-1/2}(k_h a) + \frac{2j-1}{6j+9} j_{j-1/2}(k_- a)j_{j+3/2}(k_h a) \right] \\ - \frac{j_{j+1/2}(k_c a)j_{j-1/2}(k_- a)k_- k_+ \Lambda_h(k_+) \Lambda_s(k_-)}{\Lambda_0(k_-) \Lambda_0(k_+)} \left[j_{j+3/2}(k_+ a)j_{j-1/2}(k_h a) + \frac{2j-1}{6j+9} j_{j-1/2}(k_+ a)j_{j+3/2}(k_h a) \right] \\ + \frac{j_{j+1/2}(k_- a)j_{j-1/2}(k_c a)k_c k_+ \Lambda_h(k_+) \Lambda_s(k_c)}{\Lambda_0(k_c) \Lambda_0(k_+)} \left[j_{j+3/2}(k_+ a)j_{j-1/2}(k_h a) + \frac{2j-1}{6j+9} j_{j-1/2}(k_+ a)j_{j+3/2}(k_h a) \right] \\ - \frac{j_{j+1/2}(k_- a)j_{j-1/2}(k_+ a)k_c k_+ \Lambda_h(k_c) \Lambda_s(k_+)}{\Lambda_0(k_c) \Lambda_0(k_+)} \left[j_{j+3/2}(k_c a)j_{j-1/2}(k_h a) + \frac{2j-1}{6j+9} j_{j-1/2}(k_c a)j_{j+3/2}(k_h a) \right] \\ - \frac{j_{j+1/2}(k_+ a)j_{j-1/2}(k_c a)k_c k_- \Lambda_h(k_-) \Lambda_s(k_c)}{\Lambda_0(k_c) \Lambda_0(k_-)} \left[j_{j+3/2}(k_- a)j_{j-1/2}(k_h a) + \frac{2j-1}{6j+9} j_{j-1/2}(k_- a)j_{j+3/2}(k_h a) \right] \\ + \frac{j_{j+1/2}(k_+ a)j_{j-1/2}(k_- a)k_c k_- \Lambda_h(k_c) \Lambda_s(k_-)}{\Lambda_0(k_c) \Lambda_0(k_-)} \left[j_{j+3/2}(k_c a)j_{j-1/2}(k_h a) + \frac{2j-1}{6j+9} j_{j-1/2}(k_c a)j_{j+3/2}(k_h a) \right] = 0. \quad (34)$$

This can be rewritten, as for the even states, using the condition $|k_c|a \gg 1$ and Eq. (30):

$$\begin{aligned}
& (1-3\eta_j^-) \left[\frac{\Lambda_s(k_+)}{\Lambda_h(k_+)} - \frac{\Lambda_s(k_-)}{\Lambda_h(k_-)} \right] j_{j-1/2}(k_+a) j_{j-1/2}(k_-a) j_{j+3/2}(k_ha) - 3(1+\eta_j^-) j_{j-1/2}(k_ha) \\
& \times \left[\frac{\Lambda_s(k_-)}{\Lambda_h(k_-)} j_{j-1/2}(k_-a) j_{j+3/2}(k_+a) - \frac{\Lambda_s(k_+)}{\Lambda_h(k_+)} j_{j-1/2}(k_+a) j_{j+3/2}(k_-a) \right] \\
& = \frac{\alpha}{|\alpha|} \sqrt{\frac{\alpha}{v^2(\gamma_1+4\gamma)}} \frac{\Lambda_0(k_-)}{k_- \Lambda_h(k_-)} \left\{ (1-3\eta_j^-) \left[1 - \frac{\Lambda_s(k_+)}{\Lambda_h(k_+)} \right] j_{j+1/2}(k_-a) j_{j-1/2}(k_+a) j_{j+3/2}(k_ha) \right. \\
& \quad \left. + 3(1+\eta_j^-) j_{j-1/2}(k_ha) j_{j+1/2}(k_-a) \left[j_{j+3/2}(k_+a) + \frac{\Lambda_s(k_+)}{\Lambda_h(k_+)} j_{j-1/2}(k_+a) \right] \right\} \\
& \quad - \frac{\alpha}{|\alpha|} \sqrt{\frac{\alpha}{v^2(\gamma_1+4\gamma)}} \frac{\Lambda_0(k_+)}{k_+ \Lambda_h(k_+)} \left\{ (1-3\eta_j^-) \left[1 - \frac{\Lambda_s(k_-)}{\Lambda_h(k_-)} \right] j_{j+1/2}(k_+a) j_{j-1/2}(k_-a) j_{j+3/2}(k_ha) \right. \\
& \quad \left. + 3(1+\eta_j^-) j_{j+1/2}(k_+a) j_{j-1/2}(k_ha) \left[j_{j+3/2}(k_-a) + \frac{\Lambda_s(k_-)}{\Lambda_h(k_-)} j_{j-1/2}(k_-a) \right] \right\}. \tag{35}
\end{aligned}$$

This equation describes the energies of both the electron and hole odd states. If $\alpha=0$ the equation becomes the equation for the hole states in the six-band model, but now also takes the nonparabolicity of the light hole into account. Again, the second term on the right hand side of the equation is much smaller than the first one.

Following a similar procedure to that for the even states, we can obtain from Eq. (35) the equation for the electron odd states:

$$\begin{aligned}
j_{j+1/2}(k_-a) &= \frac{1}{4[1-\Lambda_s(k_+)/\Lambda_h(k_+)]} \frac{\alpha}{|\alpha|} \sqrt{\frac{v^2(\gamma_1+4\gamma)}{\alpha}} \frac{k_- \Lambda_h(k_-)}{\Lambda_0(k_-)} \left\{ -3(1+\eta_j^-) \frac{\Lambda_s(k_+)}{\Lambda_h(k_+)} j_{j+3/2}(k_-a) - j_{j-1/2}(k_-a) \right. \\
& \times \left[\frac{4\Lambda_s(k_-)}{\Lambda_h(k_-)} - (1-3\eta_j^-) \frac{\Lambda_s(k_+)}{\Lambda_h(k_+)} \right] \left. - \frac{k_- \Lambda_h(k_-) \Lambda_0(k_+)}{|k_+| \Lambda_0(k_-) \Lambda_h(k_+)} \frac{3}{4[1-\Lambda_s(k_+)/\Lambda_h(k_+)]} \right\} j_{j-1/2}(k_-a) \\
& \times \left[\frac{4}{3} \left(\frac{\Lambda_s(k_-)}{\Lambda_h(k_-)} - 1 \right) + (1+\eta_j^-) \right] + (1+\eta_j^-) j_{j+3/2}(k_-a) \left. \right\}. \tag{36}
\end{aligned}$$

In the uncoupled case, when $\gamma_1+4\gamma=0$, Eqs. (36) and (32) are identical. The splitting of the electron levels is determined by the coupling with the valence band. Of the two terms on the right hand side of this equation, which describe the coupling with the valence band, the second is always much smaller than the first.

Equations (32) and (36) clearly show that the coupling of the electron levels with the valence band is determined by the parameter $(\gamma_1+4\gamma)/\alpha$, and, conversely, Eqs. (31) and (35) show that the effect of the conduction band on the hole level positions is determined by its inverse $\alpha/(\gamma_1+4\gamma)$. Before calculating the QSL's in several particular semiconductor nanocrystals, we will analyze more closely, in the limit $\Delta=0$, the parameters that effect the coupling and the effect of the coupling on the quantum size levels.

B. The case $\Delta=0$

For all energies $|E| \gg \Delta$ ($|\varepsilon| \gg \delta$), Eq. (25) gives $k_+^2(\gamma_1-2\gamma) \approx -\varepsilon-2\delta/3$; substituting k_+^2 into Eq. (28) gives

$$\begin{aligned}
\Lambda_h(k_+) &\approx \delta/3, \quad \Lambda_s(k_+) \approx -2\delta/3, \\
\Lambda_0(k_+) &\approx -2\delta^2/9. \tag{37}
\end{aligned}$$

On the other hand, using the conditions $v^2 \gg |(\varepsilon-\varepsilon_g)(\gamma_1+4\gamma)|$, $|\varepsilon\alpha|$, one obtains from Eq. (25):

$$\frac{\Lambda_0(k_-)}{k_- \Lambda_h(k_-)} \approx \frac{\varepsilon}{|\varepsilon|} \sqrt{\frac{v^2 \varepsilon}{\varepsilon-\varepsilon_g}}, \quad \frac{\Lambda_s(k_-)}{\Lambda_h(k_-)} \approx 1, \tag{38}$$

where we used $k_-^2 \approx \varepsilon(\varepsilon-\varepsilon_g)/v^2$ and $(\gamma_1-2\gamma)k_-^2 + \varepsilon \approx \varepsilon$. Substituting Eqs. (37) and (38) into Eqs. (31) and (35) for the hole levels, we find that for $\Delta=0$ the level energies are determined by two equations:

$$j_{j+1/2}(k_ha) = 0, \tag{39}$$

and

$$\begin{aligned}
& j_{j+1/2}(k-a)j_{j-3/2}(k_h a) + \frac{1-\eta_j^+}{1+\eta_j^+} j_{j+1/2}(k_h a)j_{j-3/2}(k-a) \\
&= -\frac{\alpha}{|\alpha|} \sqrt{\frac{\Delta E_h \alpha}{(E_g + \Delta E_h)(\gamma_1 + 4\gamma)}} j_{j-1/2}(k-a) \left[j_{j-3/2}(k_h a) - \frac{1-\eta_j^+}{1+\eta_j^+} j_{j+1/2}(k_h a) \right], \quad (40)
\end{aligned}$$

which are valid for all j starting from $j = \frac{1}{2}$ and where $E_g = \hbar^2 \varepsilon_g / 2m_0$ and $\Delta E_h = -\hbar^2 \varepsilon / 2m_0$ is the hole level energy measured from the top of the valence band. By the same procedure we get two equations from Eq. (35) for the odd hole states for $\Delta = 0$:

$$j_{j-1/2}(k_h a) = 0, \quad (41)$$

which is valid for all $j > \frac{1}{2}$, and

$$\begin{aligned}
& j_{j-1/2}(k_h a)j_{j+3/2}(k-a) + \frac{1-\eta_j^-}{1+\eta_j^-} j_{j-1/2}(k-a)j_{j+3/2}(k_h a) \\
&= -\frac{\alpha}{|\alpha|} \sqrt{\frac{\Delta E_h \alpha}{(E_g + \Delta E_h)(\gamma_1 + 4\gamma)}} j_{j+1/2}(k-a) \left[j_{j-1/2}(k_h a) - \frac{1-\eta_j^-}{1+\eta_j^-} j_{j+3/2}(k_h a) \right], \quad (42)
\end{aligned}$$

which is valid for all j starting from $j = \frac{1}{2}$. If we replace j by $j+1$ in Eq. (40) for the even states, it becomes identical to Eq. (42) for the odd states. This means that all hole levels for $\Delta = 0$ have a degree of degeneracy greater than 6, except the even state with $j = \frac{1}{2}$, which is only twofold degenerate. Finite Δ lifts this degeneracy.

It is important to note that the admixture of the conduction band into the valence band is determined not only by the natural energy parameter $\Delta E_h / (E_g + \Delta E_h)$, the ratio of the quantization energy to the energy gap, but also by the ratio $\alpha / (\gamma_1 + 4\gamma)$ (actually by their square roots). This latter ratio then could produce quite large an admixture even if the confinement energy were much smaller than the energy gap, or, conversely, considerably decrease the admixture even though $\Delta E_h > E_g$.

Substituting Eqs. (37) and (38) into Eqs. (32) and (36), for the electron quantum size levels we obtain for the even states:

$$\begin{aligned}
j_{j-1/2}(k-a) &= \frac{1}{2} \frac{\alpha}{|\alpha|} \sqrt{\frac{\Delta E_e (\gamma_1 + 4\gamma)}{(E_g + \Delta E_e) \alpha}} \\
&\times [(1 + \eta_j^+) j_{j+1/2}(k-a) \\
&- (1 - \eta_j^+) j_{j-3/2}(k-a)], \quad (43)
\end{aligned}$$

where the electron level energies, $\Delta E_e = \hbar^2 (\varepsilon - \varepsilon_g) / 2m_0$, are measured from the bottom of the conduction band. The second term in the right side of Eq. (32) is a correction term that is proportional to Δ , and may be written for $j > \frac{1}{2}$:

$$\begin{aligned}
&\sim -\frac{\Delta}{6(E_g + \Delta E_e)} \sqrt{\frac{\Delta E_e (\gamma_1 - 2\gamma)}{E_p}} (1 - \eta_j^+) \\
&\times [j_{j+1/2}(k-a) + j_{j-3/2}(k-a)]. \quad (44)
\end{aligned}$$

For $j = \frac{1}{2}$ it is proportional to Δ^2 . The same procedure for the odd electron states gives:

$$\begin{aligned}
j_{j+1/2}(k-a) &= \frac{1}{2} \frac{\alpha}{|\alpha|} \sqrt{\frac{\Delta E_e (\gamma_1 + 4\gamma)}{(E_g + \Delta E_e) \alpha}} \\
&\times [(1 + \eta_j^-) j_{j+3/2}(k-a) \\
&- (1 - \eta_j^-) j_{j-1/2}(k-a)]. \quad (45)
\end{aligned}$$

The second term in the right-hand side of Eq. (36) is a correction proportional to Δ :

$$\begin{aligned}
&\sim \frac{\Delta}{6(E_g + \Delta E_e)} \sqrt{\frac{\Delta E_e (\gamma_1 - 2\gamma)}{E_p}} (1 + \eta_j^-) \\
&\times [j_{j+3/2}(k-a) + j_{j-1/2}(k-a)]. \quad (46)
\end{aligned}$$

As before, Eq. (43) for the even states becomes identical to Eq. (45) if we replace j by $j+1$. This shows that all electron levels for $\Delta = 0$, even though they are coupled with the valence band, have the same degree of degeneracy as in a simple parabolic band model [the $1S(e)$ electron level is twofold degenerate, the $1P(e)$ is six-fold degenerate, etc., taking electron spin into account]. Finite Δ gives corrections having different signs in Eqs. (43) and (45), and lifts this degeneracy. As a result the $1P(e)$ electron level is split into $1P_{3/2}(e)$ and $1P_{1/2}(e)$ states.

As for the admixture of the conduction band into the valence band, the admixture of the valence band into the conduction band is also determined not only by the natural energy parameter $\Delta E_e / (E_g + \Delta E_e)$, the ratio of the electron quantization energy to the energy gap, but also by $(\gamma_1 + 4\gamma) / \alpha$. This latter parameter can make the admixture large even if the confinement energy is much smaller than the energy gap, or, conversely, can greatly decrease the admixture even if $\Delta E_e > E_g$. This parameter is the inverse of the one affecting the admixture of the conduction band in the hole levels. So even if the effect of the valence band on the conduction state is ‘‘strong,’’ the effect of the conduction band on the hole levels may be ‘‘weak,’’ and vice versa.

In order to illustrate the role of the coupling, we calculated the size dependence of the lowest hole and electron

levels in ‘‘InP semiconductor’’ nanocrystals using $\Delta = 0$, (this approximation is reasonable because Δ is only 110 meV in InP), and compare these results with calculations done using other techniques. The energy parameters we used are: $E_g = 1.424$ eV, $E_p = 20.6$ eV, $f = -1.1$, $\gamma_1^L = 5.25$, and $\gamma^L = (2\gamma_2^L + 3\gamma_3^L)/5 = 1.9$,²⁴ which result in $\alpha = -1.2$, $\gamma_1 = 0.41$, and $\gamma = -0.51$. We will also calculate the size dependence using another set of the parameters $\gamma_1 + 4\gamma$, α , and E_p , now with $\alpha > 0$ and $\gamma_1 + 4\gamma > 0$, but keeping the effective masses of the electron, $m_0(\alpha + E_p/E_g)^{-1}$, light hole, $m_0(\gamma_1 + 4\gamma + E_p/E_g)^{-1}$, and heavy hole $m_0(\gamma_1 - 2\gamma)^{-1}$ the same as measured in bulk.

In parabolic band approximation the energy of the $1S(e)$ electron level is determined by the simple expression: $\Delta E_e = \hbar^2 k_-^2 / 2m_e = \hbar^2 \pi^2 / 2m_e a^2$, where $k_- = \pi/a$ and where $m_e = m_0 / (\alpha + E_p/E_g)$ is the effective mass of the electron at the bottom of the conduction band with $\Delta = 0$ [see Eq. (4)]. In the uncoupled case, ($\gamma_1 = \gamma = 0$), Eq. (43) for $j = \frac{1}{2}$ again gives $k_- = \pi/a$; however, the energy dependence of the effective mass $m_e(\Delta E_e)$ is taken into account [see Eq. (7)] and

$$\Delta E_e = \frac{\hbar^2 k_-^2}{2m_e(\Delta E_e)} = \frac{\hbar^2 \pi^2}{2m_0 a^2} \left(\alpha + \frac{E_p}{E_g + \Delta E_e} \right). \quad (47)$$

This expression was the one used for the electron QSL’s in Ref. 11. One sees that the electron effective mass increases with the energy of the levels. Since the position of the level is inversely proportional to the effective mass, the energy dependence of the effective mass slows down the shift of the level with the size [see Fig. 2(a)]. In the full eight-band PB model, k_- is related to the energy almost in the same way as in the Kane model. However, for any finite ΔE_e , when the right side of Eq. (43) is nonzero and $\alpha > 0$, the solution of this equation gives $k_- a < \pi$. This leads to a still further slowing down of the size dependence of the electron levels with decreasing size as shown in Fig. 2(a). If $\alpha < 0$ the root $k_- a$ is greater than π resulting in the shift of the $1S(e)$ electron level to higher energy.

There are two equations, Eqs. (39) and (40), for the hole levels for $\Delta = 0$. The first determines the QSLs of heavy holes only and does not couple with the conduction band. The lowest hole level [the $1P_{1/2}(h)$ state] has p -symmetry and its energy is given by Eq. (39) with $j = \frac{1}{2}$:

$$\Delta E_h(1P_{1/2}) = \frac{\hbar^2 (4.49)^2}{2m_{hh} a^2}, \quad (48)$$

where $m_{hh} = m_0 / (\gamma_1^L - 2\gamma^L) = m_0 / (\gamma_1 - 2\gamma)$ is the heavy-hole effective mass. However, selection rules do not allow transitions from this level to the ground $1S(e)$ electron quantum size level, because of the different symmetries of their envelope wave functions.^{10,11}

Hole states with mixed s - d symmetry, from which transitions to the first electron quantum size level are allowed, are described by Eq. (40) with $j = \frac{3}{2}$. In parabolic approximation and $\Delta = 0$ their energies are determined by setting the right side of this equation to zero:

$$2j_0(k_h a)j_2(\sqrt{\beta}k_h a) + j_0(\sqrt{\beta}k_h a)j_2(k_h a) = 0, \quad (49)$$

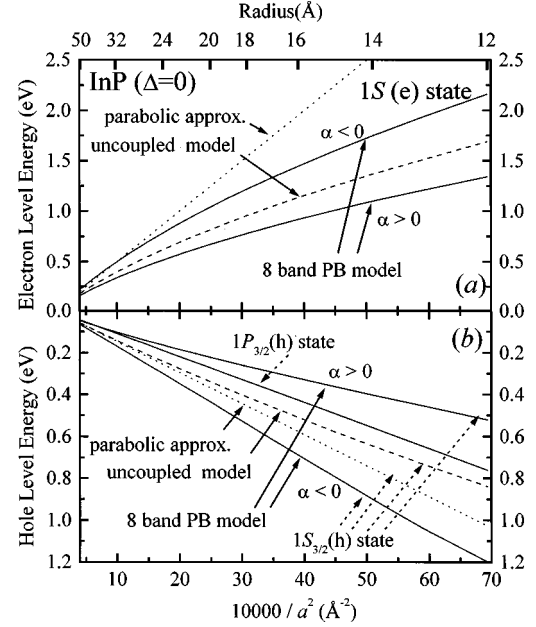


FIG. 2. Size dependence of the lowest QSL’s in InP nanocrystals, with $\Delta = 0$, calculated using different approximations: (a) the $1S_e$ electron level and (b) the $1P_{1/2}(h)$ and $1S_{3/2}(h)$ hole levels. Dotted lines show the results of calculations within the simple parabolic approximation for the conduction band and the Luttinger-Kohn parabolic approximation for the valence band. Dashed lines show the effect of the nonparabolicity of the electron- and light-hole spectra without taking the coupling of the conduction and valence bands into account. Solid lines show the results of the calculations done within the eight-band Pidgeon and Brown model for the set of energy band parameters discussed in the text for $\alpha > 0$ and $\alpha < 0$. The size dependence of the $1P_{3/2}(h)$ hole state is the same for all these models.

where $k_h^2 = 2m_0 \Delta E_h / [\hbar^2 (\gamma_1^L - 2\gamma^L)]$, $k_-^2 = 2m_0 \Delta E_e / [\hbar^2 (\gamma_1^L + 4\gamma^L)]$, and $\beta = k_-^2 / k_h^2 = (\gamma_1^L - 2\gamma^L) / (\gamma_1^L + 4\gamma^L)$. The values of $k_h a$, which solve this equation, depend only on β . In InP $\beta = 0.115$ and the solution of Eq. (49) gives $k_h a \approx 5.21$. The energy of the first hole state with mixed s - d symmetry (the $1S_{3/2}$ state) when $\Delta = 0$ is then

$$\Delta E_h(1S_{3/2}) = \frac{\hbar^2 k_h^2}{2m_{hh}} = \frac{\hbar^2 (5.21)^2}{2m_{hh} a^2}. \quad (50)$$

Comparison of Eqs. (48) and (50) shows that the ground-hole state in InP nanocrystals has p -type symmetry in parabolic approximation [see also Fig. 2(b)]. This level order is consistent with the prediction of the six-band model for InP nanocrystals.²⁵ Studying the dependence of the solutions of Eq. (49) on β shows that for $\Delta = 0$ the level order changes when $\beta > 0.215$, and that the $1S_{3/2}(h)$ state then becomes the ground-hole state.

In the uncoupled case, when $\alpha = 0$, the energies of the hole levels are determined by setting of the left side of Eq. (40) to zero; however, this now takes the nonparabolicity of the light hole into account. The hole energies are then determined by Eq. (49) where $\beta(\Delta E_h)$ is now a function of the energy of the state:

$$\begin{aligned}\beta(\Delta E_h) &= \frac{\gamma_1 - 2\gamma}{\gamma_1^L(\Delta E_h) + 4\gamma^L(\Delta E_h)} \\ &= \frac{\gamma_1 - 2\gamma}{\gamma_1 + 4\gamma + E_p/(E_g + \Delta E_h)}.\end{aligned}\quad (51)$$

Figure 2(b) shows that the nonparabolicity of the light hole slows the $1/a^2$ dependence of the $1S_{3/2}(h)$ hole-state energies. For holes, if we take coupling with the conduction band into account, for finite $\alpha > 0$ and ΔE_h , i.e., when the right-hand side of Eq. (42) is nonzero and negative, then the solution of this equation gives values of k_-a smaller than those found from Eq. (49). This leads to a further slowing down of the size dependence of the hole levels with decreasing size. Figure 2(b) shows this dependence for the parameters $\alpha = 0.63$, $\gamma_1 = 1.04$, $\gamma = -0.21$, and $E_p = 18.0$, which keep the effective carrier masses equal to those measured in bulk InP. For these parameters the $1S_{3/2}(h)$ level crosses the $1P_{1/2}(h)$ level and becomes the ground-hole state for nanocrystal radii less than 35 Å. This agrees with the results of pseudopotential calculations made for small InP nanocrystals.²⁶ Negative α leads to an increase of k_-a , and to a ground state that has p -type symmetry. The corresponding results, calculated for energy parameters from Ref. 24, $\alpha = -1.2$, $\gamma_1 = 0.41$, $\gamma = -0.51$, and $E_p = 20.6$, are shown in Fig. 2(b).

The analysis presented above shows how sensitive the absorption spectra are to the energy-band parameters. The structure and positions of the quantum size levels in small nanocrystals are determined not by the values of the effective masses at the bottom of the conduction band and at the top of the valence band alone. They strongly depend on the relative contribution of the remote bands and the nearest band. The drastic change of the level structure presented in Fig. 2 is obtained by changing E_p only by 10%.

IV. SIZE DEPENDENCE OF QUANTUM SIZE LEVELS IN SEVERAL SAMPLE SEMICONDUCTOR NANOCRYSTALS

We will calculate the size dependence of the quantum size levels in wide gap CdS, moderate gap CdTe, and narrow gap InSb nanocrystals. CdS and CdTe are selected because nanocrystal samples of these materials have already been prepared and size selective spectroscopy of their quantum confined levels can be studied experimentally. Comparison of the results obtained in the eight-band PB model with those obtained in the uncoupled model shows that, although the uncoupled six-band model gives the same level order as the eight-band model and qualitatively describes the structure of absorption spectra, the coupling is important for a quantitative description of the levels even in wide gap CdS. A description of the absorption level structure of narrow gap InSb can be done only in the eight-band PB model, because coupling between the conduction and the valence bands is always important in narrow gap semiconductors and the uncoupled six-band model gives wrong results even in relatively large nanocrystals.²⁷ For each semiconductor we show the size dependences only for the range of energies such that the eight-band PB model validly describes its band structure.

We have shown above that quantum level structure is

very sensitive to the bulk energy band parameters. In general, these parameters are quite well determined for almost all semiconductor materials (see, for example, Refs. 16 and 28). However, energy band parameters measured in the bulk include some contributions that are absent in nanocrystals. As a result, using these parameters requires taking special precautions. For example, in narrow gap semiconductors these parameters include the correction connected with the nonlocal character of the self-consistent potential; the magnitude of these corrections is comparable with the contribution of remote bands to the electron- and hole-effective masses.²⁹ The nonlocal contributions have the form

$$\begin{aligned}\Delta\gamma_1 &= -5\delta_{nl}, & \Delta\gamma &= -4\delta_{nl}, \\ \Delta\alpha &= -10\delta_{nl}, & \delta_{nl} &= \frac{2}{15\pi\kappa E_g} \sqrt{\frac{E_B E_p}{3}},\end{aligned}\quad (52)$$

where $E_B = 27.2$ eV is the Bohr energy and κ is the dielectric constant. A different mechanism of band parameter ‘‘renormalization’’ is dominant in wide and moderate gap semiconductors. These semiconductors are usually quite polar and charged-free carriers interact strongly with polar phonons to form polarons.³⁰ As a result, in most cases the effective masses measured in bulk wide gap semiconductors are not those of free electrons and holes, but are the effective masses of the corresponding polarons (see for example Ref. 31). Both these corrections must be subtracted from the remote band contribution when one calculates the quantum levels within the eight-band model.

The following set of the bulk parameters describes the energy band structure of bulk InSb: $E_g = 0.2368$ eV, $\Delta = 0.810$ eV, $E_p = 23.42$ eV, $\gamma_2^L = 15.96$, $\gamma_3^L = 16.99$ [$\gamma^L = (2\gamma_2^L + 3\gamma_3^L)/5 = 16.58$], $\gamma_1^L = 36.41$, and $m_e = 0.0139m_0$, which results in $\alpha = -0.36$, $\gamma_1 = 3.44$, and $\gamma = 0.196$.³² These parameters do not yet allow for the nonlocal corrections described in Eq. (52). For InSb, using $\kappa = 18.3$, we find $\delta_{nl} = 0.214$, which finally leads to the remote band contributions $\gamma_1 = 4.51$, $\gamma = 0.953$, and $\alpha = 0.77$. The level structure calculated with these parameters in InSb nanocrystals is shown in Fig. 3. The most interesting effect in this spectrum is the strong splitting of the $1P(e)$ electron level into two $1P_{1/2}(e)$ and $1P_{3/2}(e)$ states. One can see in Fig. 3(b) that the $1P_{3/2}(h)$ hole state becomes the hole ground state in nanocrystals smaller than 60 Å in radius. The rapid changes in the size dependence of the $1S_{3/2}(h)$ and $2S_{3/2}(h)$ hole states in the energy region close to Δ reflect anticrossings similar to those observed in CdSe for $S_{1/2}(h)$ states.³

We use the following set of bulk energy band parameters to describe CdTe: $E_g = 1.6069$ eV, $\Delta = 0.953$ eV, $\gamma_1^L = 5.37$, $\gamma_2^L = 1.67$, $\gamma_3^L = 1.98$, [$\gamma^L = (2\gamma_2^L + 3\gamma_3^L)/5 = 1.86$], $m_e = 0.091m_0$, from Ref. 31 and a value of the nonparabolicity parameter $E_p = 17.9$ eV.³³ This results in $\alpha = 1.24$, $\gamma_1 = 1.66$, and $\gamma = 0$, which we used to calculate the QSL’s in CdTe nanocrystals shown in Fig. 4. The splitting of the $1P(e)$ electron state is considerably smaller than in InSb, and the $1S_{3/2}(h)$ state is the ground hole state having mixed s - d symmetry. The difference is connected with the small value of E_g in InSb. Another interesting aspect of the CdTe

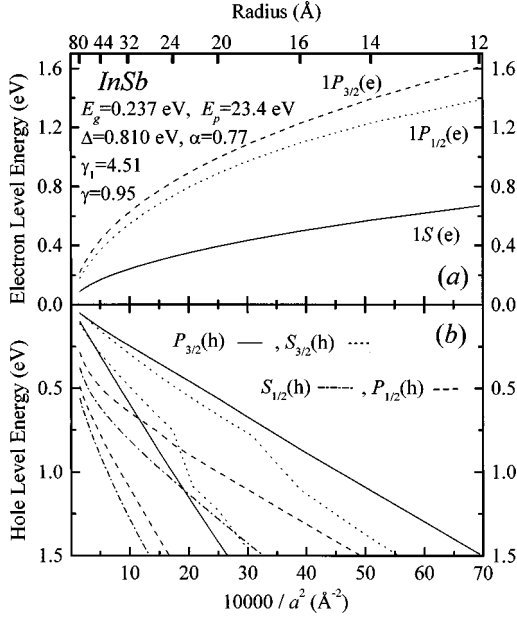


FIG. 3. Size dependence of the lowest QSL's in InSb nanocrystals: (a) the $1S_e$ and $1P_{1/2,3/2}(e)$ electron levels and (b) the two lowest hole levels for each symmetry: $P_{3/2}(h)$, $S_{3/2}(h)$, $1S_{1/2}(h)$, and $P_{1/2}(h)$.

hole level structure is the absence of jumps in the size dependence connected with an anticrossing of the $S_{3/2}(h)$ and $1S_{1/2}(h)$ levels.

For CdS we use the following set of the bulk band parameters $E_g = 2.58$ eV and $\Delta = 0.0624$ eV,¹⁹ the parameters $\gamma^I = 0.41$ and $\gamma_1^I = 1.02$ were extracted from the effective masses of the holes¹⁹ using a quasicubic model of CdS. Using the value for the electron effective mass at the bottom of the conduction band of $m_e = 0.205m_0$,¹⁹ and $E_p = 21.0$ eV,³⁴

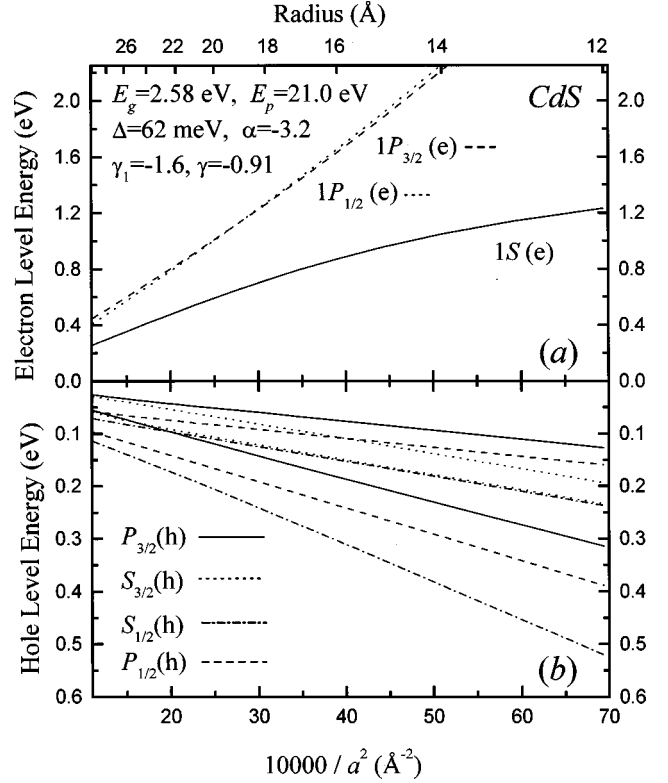


FIG. 5. Size dependence of the lowest QSL's in CdS nanocrystals: (a) the $1S_e$ and $1P_{1/2,3/2}(e)$ electron levels and (b) the two lowest hole levels for each symmetry: $P_{3/2}(h)$, $S_{3/2}(h)$, $1S_{1/2}(h)$, and $P_{1/2}(h)$.

we obtain $\alpha = -3.2$, $\gamma = -0.91$, and $\gamma_1 = -1.6$. The results of the calculation are shown in Fig. 5. One can see that the ground hole state in CdS nanocrystals has p -type symmetry as was predicted in the uncoupled six-band model.¹⁰ Although the level order is the same as that obtained in the uncoupled model, the positions of the electron and hole levels calculated with the eight-band model are quite different in small CdS nanocrystals.

V. DISCUSSION

We have developed an analytical theory of the quantum size levels in the eight-band PB model in spherical semiconductor nanocrystals having an infinite potential barrier at the crystal surface. The theory shows that the coupling between the conduction and valence bands strongly modifies the positions of the QSL's even in semiconductor nanocrystals with a relatively wide energy gap. This is because the coupling is determined by the square root, $\sqrt{\Delta E_{e,h}/(E_g + \Delta E_{e,h})}$, of the natural energy parameter: the ratio of the quantization energy $\Delta E_{e,h}$ to the energy gap E_g . Even if the quantization energy is much smaller than the energy gap the square root dependence greatly magnifies the role of the coupling. This effect should be more significant for electrons than for holes because usually we have $\Delta E_e > \Delta E_h$.

Another unexpected result is the sensitivity of the coupling to the ratio of remote band contributions to the electron and light hole effective masses, α and $\gamma_1 + 4\gamma$, respectively. The coupling is proportional to $\sqrt{(\gamma_1 + 4\gamma)/\alpha}$ for electrons

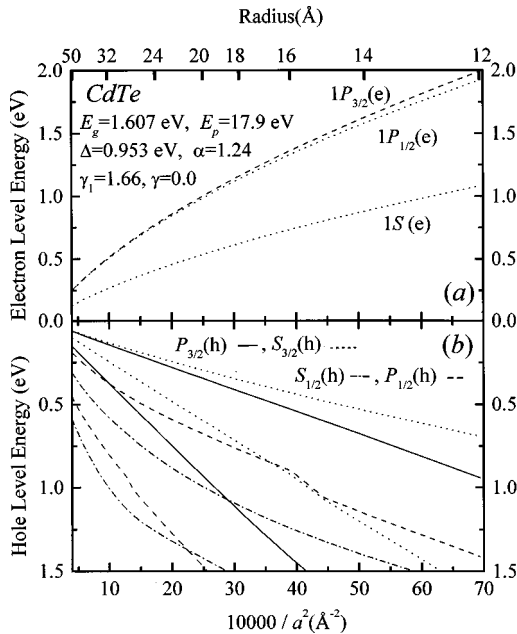


FIG. 4. Size dependence of the lowest QSL's in CdTe nanocrystals: (a) the $1S_e$ and $1P_{1/2,3/2}(e)$ electron levels and (b) the two lowest hole levels for each symmetry: $P_{3/2}(h)$, $S_{3/2}(h)$, $1S_{1/2}(h)$, and $P_{1/2}(h)$.

and to the inverse value of this ratio for holes. This parameter can considerably reduce the magnitude of the coupling for one type of the carrier, allowing one to consider the levels for these carriers independently, but, at the same time, result in a strong coupling effect for the other carrier in this case.

Optical properties of nanocrystals are determined by transitions between the electron and hole quantum confined levels. The energy of these transitions, however, are reduced by the energy of the electron-hole Coulomb interaction, which in parabolic mass approximation is equal to $-1.8e^2/\kappa a$.⁷ Although this correction is always smaller than the confinement energy in small nanocrystals, it grows as $1/a$ and its value is on the order of 100 meV in smallest nanocrystals if one uses a typical value for the static dielectric constant of $\kappa \sim 10$. However, the Coulomb interaction between the electron and hole in small nanocrystals is not described by the static dielectric constant. For one, the electronic (high frequency) component of the polarizability decreases as a result of the blueshift of the energy gap with decreasing size in nanocrystals.³⁵⁻³⁷ Also, the optical phonon contribution to the polarizability decreases with size, because the optical phonon polarization cannot follow the rapid motion of strongly quantized carriers. Both these effects lead to a decrease of the effective dielectric constant and considerably increase the electron-hole Coulomb interaction in nanocrystals, leading to an additional decrease in the transition energies.

Another important effect leads to a *size dependent renormalization* of the energy gap in small size nanocrystals. Effective mass approximation, as well as pseudopotential local-density approximation, tight binding, etc., calculations do not take into account the nonlocal character of the effective self-consistent potential acting on electrons and holes in semiconductors. This nonlocality is connected with the electron-electron exchange interaction and reduces to a local potential only for completely filled bands. The role of this effect on energy bands renormalization was first pointed out by Halperin and Rice for gapless semiconductors³⁸ and later by Gel'mont for semiconductors with a finite energy gap.³⁹ The coupling between the conduction and valence bands we have considered above, which is increasingly important in small

nanocrystals, results in a nonlocal exchange potential and therefore should lead to a size dependent renormalization of the energy gap.

Both these effects, a decrease of the dielectric constant and a nonlocal renormalization of the energy gap, can change the transition energy between electron and hole quantum confined levels as much as several hundred meV. The absence of a reliable theory of these effects makes an absolute description of the nanocrystal absorption spectra difficult. However, the separation between the hole levels, which can be extracted from the transitions to the same electron level, can be directly compared with result of our calculations. That is why the level differences seen in the photoluminescence excitation spectra in CdSe (Ref. 3) and InAs nanocrystals²⁷ were described so well, while the size dependence of absorption spectra in the smallest nanocrystals differed from the theoretical predictions.

In summary, we have developed an analytical theory of the quantum size levels in a spherical eight-band Pidgeon and Brown model for nanocrystals surrounded by an infinite potential barrier. This theory of the quantum size levels explicitly includes the mixing between the conduction and valence bands and the degeneracy of the valence band and naturally generalizes all previous considerations. It is shown that the mixing can be important even in relatively wide gap semiconductor nanocrystals, because it is governed by the square root of the ratio of the quantization energy to the energy gap, and should always be taken into account in narrow gap semiconductors. Calculations made for several particular semiconductor nanocrystals demonstrate a sensitivity of the level structure to the contribution of remote bands to effective masses of the electrons and light holes. The ratio of these contributions determines the mixing of the conduction band into the hole levels, and its inverse determines the mixing of the valence band in the electron levels.

ACKNOWLEDGMENTS

We would like to thank Peter Sercel for his important comments on our unpublished manuscript, and R. P. Seisyan for information on the energy band parameters. This work was supported by the Office of Naval Research.

¹L. E. Brus, Appl. Phys. A: Solids Surf. **53**, 465 (1991).

²A. P. Alivisatos, Science **271**, 933 (1996).

³D. J. Norris and M. G. Bawendi, Phys. Rev. B **53**, 16 338 (1996).

⁴S. Schmitt-Rink, D. A. B. Miller, and D. S. Chemla, Phys. Rev. B **35**, 8113 (1987).

⁵P. Horan and W. Blau, Phase Transit. **24-26**, 605 (1990).

⁶Al. L. Efros and A. L. Efros, Sov. Phys. Semicond. **16**, 772 (1982).

⁷L. E. Brus, J. Chem. Phys. **79**, 5566 (1983).

⁸A. I. Ekimov, A. A. Onushchenko, A. G. Plukhin, and Al. L. Efros, Zh. Eksp. Teor. Fiz. **88**, 1490 (1985) [Sov. Phys. JETP **61**, 891 (1985)].

⁹J. B. Xia, Phys. Rev. B **40**, 8500 (1989).

¹⁰G. B. Grigoryan, E. Kazaryan, Al. L. Efros, and T. V. Yazeva, Sov. Phys. Solid State **32**, 1031 (1990).

¹¹A. I. Ekimov, F. Hache, M. C. Schanne-Klein, D. Ricard, C. Flytzanis, I. A. Kudryavtsev, T. V. Yazeva, A. V. Rodina, and Al. L. Efros, J. Opt. Soc. Am. B **10**, 100 (1993).

¹²D. J. Norris, A. Sacra, C. B. Murray, and M. G. Bawendi, Phys. Rev. Lett. **72**, 2612 (1994).

¹³A. I. Ekimov, Phys. Scr. **39**, 217 (1991); Radiat. Eff. Defects Solids **134**, 11 (1995).

¹⁴P. A. M. Rodrigues, G. Tamulaitis, S. H. Risbud, and P. Y. Yu, Solid State Commun. **94**, 583 (1995).

¹⁵C. R. Pidgeon and R. N. Brown, Phys. Rev. **146**, 575 (1966).

¹⁶R. L. Aggarwal, in *Modulation Techniques*, edited by P. K. Willardson and A. C. Beer, Semiconductor and Semimetals Vol. 9 (Academic, New York, 1974), p. 151.

¹⁷P. C. Sercel and K. J. Vahala, Phys. Rev. B **42**, 3690 (1990); K. J. Vahala and P. C. Sercel, Phys. Rev. Lett. **65**, 239 (1990).

- ¹⁸I. Kang and F. Wise, *J. Opt. Soc. Am. B* **14**, 1632 (1997).
- ¹⁹G. L. Bir and G. E. Pikus, *Symmetry and Strain-Induced Effects in Semiconductors* (Wiley, New York, 1975).
- ²⁰E. O. Kane, *J. Phys. Chem. Solids* **1**, 249 (1956).
- ²¹B. L. Gel'mont and M. I. D'yakonov, *Fiz. Tekh. Poluprovodn.* **5**, 2191 (1971) [*Sov. Phys. Semicond.* **5**, 1905 (1972)].
- ²²V. I. Sheka and D. I. Sheka, *Zh. Eksp. Teor. Fiz.* **51**, 1445 (1966) [*Sov. Phys. JETP* **24**, 975 (1967)].
- ²³A. R. Edmonds, *Angular Momentum in Quantum Mechanics* (Princeton University Press, Princeton, New Jersey, 1957).
- ²⁴S. I. Kokhanovskii, Y. M. Makushenko, R. P. Seisyan, Al. L. Efros, T. V. Yazeva, and M. A. Abdullaev, *Fiz. Tverd. Tela (Leningrad)* **33**, 1719 (1991) [*Sov. Phys. Solid State* **33**, 967 (1991)].
- ²⁵T. Richard, P. Lefebvre, H. Mathieu, and J. Allegre, *Phys. Rev. B* **53**, 7287 (1996).
- ²⁶O. I. Micic, H. M. Cheong, H. Fu, A. Zunger, J. R. Sprague, A. Mascarenhas, and A. J. Nozik, *J. Phys. Chem. B* **101**, 4904 (1997).
- ²⁷U. Banin, J. C. Lee, A. A. Guzelian, A. V. Kadavanich, A. P. Alivisatos, W. Jaskolski, G. Bryant, Al. L. Efros, and M. Rosen, *J. Chem. Phys.* **109**, 2036 (1998).
- ²⁸R. P. Seisyan, *Diamagnetic Exciton Spectroscopy* (Nauka, Moscow, 1984); R. P. Seisyan and B. P. Zakharchenya, in *Landau Level Spectroscopy*, edited by E. I. Rashba and G. Landwehr (North Holland, Amsterdam, 1991), Vol. 1, p. 345.
- ²⁹B. L. Gel'mont, R. P. Seisyan, and Al. L. Efros, *Fiz. Tekh. Poluprovodn.* **16**, 776 (1982) [*Sov. Phys. Semicond.* **16**, 499 (1982)].
- ³⁰J. Appel, *Solid State Phys.* **21**, 193 (1968).
- ³¹G. N. Aliev, O. S. Coschug, A. I. Nesvizskii, R. P. Seisyan, and T. V. Yazeva, *Fiz. Tverd. Tela (Leningrad)* **35**, 1514 (1993) [*Sov. Phys. Solid State* **35**, 764 (1993)].
- ³²Al. L. Efros, L. M. Kanskaya, S. I. Kokhanovskii, and R. P. Seisyan, *Solid State Commun.* **43**, 613 (1982).
- ³³M. H. Weiler, R. L. Aggarwal, and B. Lax, *Phys. Rev. B* **16**, 3603 (1978).
- ³⁴C. Hermann and C. Weisbuch, *Phys. Rev. B* **15**, 823 (1977).
- ³⁵J. F. Harvey, H. Shen, R. A. Lux, M. Dutta, J. Pamulapati, and R. Tsu, *Mater. Res. Soc. Symp. Proc.* **256**, 175 (1992).
- ³⁶K. V. Kahen, J. P. Leburton, and K. Hess, *Superlattices Microstruct.* **1**, 289 (1985).
- ³⁷L. W. Wang and A. Zunger, *Phys. Rev. Lett.* **73**, 1039 (1994).
- ³⁸B. I. Halperin and T. M. Rice, *Rev. Mod. Phys.* **40**, 755 (1960).
- ³⁹B. L. Gel'mont, *Fiz. Tekh. Poluprovodn.* **9**, 1912 (1975) [*Sov. Phys. Semicond.* **9**, 1257 (1975)].